NASA Contractor Report 195345

Isothermal Damage and Fatigue Behavior of SCS-6/Timetal 21S $[0/90]_s$ Composite at 650°C

Michael G. Castelli
NYMA, Inc.
Engineering Services Division
Brook Park, Ohio

June 1994

Prepared for
Lewis Research Center
Under Contract NAS3–27186

National Aeronautics and
Space Administration

Trade names or manufacturers' names are used in this report for identification only. This usage does not constitute an official endorsement, either expressed or implied, by the National Aeronautics and Space Administration.

ISOTHERMAL DAMAGE AND FATIGUE BEHAVIOR OF SCS-6/TIMETAL 21S $[0/90]_s$ COMPOSITE AT 650°C

Michael G. Castelli
NYMA, Inc.
Engineering Services Division
2001 Aerospace Parkway
Brook Park, Ohio 44142

ABSTRACT: The isothermal fatigue damage and life behaviors of SCS-6/Timetal 21S $[0/90]_s$ were investigated at 650°C. Strain ratchetting and degradation of the composite's static elastic modulus were carefully monitored as functions of cycles to indicate damage progression. Extensive fractographic and metallographic analyses were conducted to determine damage/failure mechanisms. Resulting fatigue lives show considerable reductions in comparison to [0] reinforced titanium matrix composites subjected to comparable conditions. Notable stiffness degradations were found to occur after the first cycle of loading, even at relatively low maximum stress levels, where cyclic lives are greater than 25,000 cycles. This was attributed to the extremely weak fiber/matrix bond which fails under relatively low transverse loads. Stiffness degradations incurred on first cycle loadings and degradations thereafter were found to increase with increasing maximum stress. Environmental effects associated with oxidation of the [90] fiber interfaces clearly played a role in the damage mechanisms as fracture surfaces revealed environment assisted matrix cracking along the [90] fibers. Metallographic analysis indicated that all observable matrix fatigue cracks initiated at the [90] fiber/matrix interfaces. Global de-bonding in the loading direction was found along the [90] fibers. No surface initiated cracks were evident and minimal if any [0] fiber cracking was visible.

KEY WORDS: titanium matrix composites; fatigue behavior; damage mechanisms; metallographic analyses, stiffness loss

INTRODUCTION

Silicon-carbon fiber reinforced titanium matrix composites (TMCs) have received considerable attention over recent years for their potential use in advanced high temperature airframe and propulsion system applications. The obvious attractions of such materials are their increased stiffness and strength/weight ratios at elevated temperatures when compared to conventional high temperature alloys. These attractions and potential benefits are clearly evident in unidirectional systems with uniaxial loading in the fiber direction. However, they become much less evident with the introduction of off-axis fibers and/or the introduction of loads not coinciding with a primary fiber direction [ref. 1].

It is evident that many of the structural applications for which TMCs are being considered will experience a variety of multiaxial loads, thus, establishing requirements of load carrying capabilities in more than one direction. Therefore, many composite materials will necessarily incorporate multiple fiber orientations, the most obvious of which include the [0] and [90] directions. High temperature testing of various TMCs containing [90] fibers has revealed that the tensile [refs. 2,3], isothermal [refs. 4-6], and thermomechanical [refs. 7-14] fatigue properties are drastically reduced from those exhibited by [0] TMCs. Much of this

degradation has been attributed to the weak bond strength at the fiber/matrix (F/M) interface, which is often assumed to either fail at extremely low stresses, or be essentially non-existent beyond that which is mechanically induced by the internal residual stress state of the composite. Thus, some degree of internal damage is immediately introduced with initial loading. In addition, environmental degradation effects are clearly exacerbated by the exposed [90] fiber ends [refs. 8,12], as oxygen can apparently diffuse easily along the F/M interfaces. This condition is likely, for example, in applications where a TMC component contains holes for mechanical fastening. Further, initial experimental studies on clad [0] TMC coupons (where external titanium cladding completely encases a TMC core with no external points of fiber exposure) [7] suggest that many of the environmental concerns remain, given the relatively high oxygen diffusivity rates of titanium alloys.

With the aforementioned complexities and concerns, it essential that the fundamental fatigue damage/failure mechanisms in TMCs are carefully characterized to guide the theoretical tools being developed to predict their mechanical behaviors under diverse loading conditions. To this end, the work presented here was undertaken to characterize the deformation, damage progression, and low cycle fatigue behaviors of a $[0/90]_s$ TMC under idealized uniaxial 650°C isothermal conditions. Particular emphasis was placed on identifying the physical damage/failure mechanisms at the microstructural level. This was accomplished by combining information gathered from optical and scanning electron microscopy (SEM) fractography and metallography on both failed and interrupted specimens. Through this information and a detailed description of the macroscopic response, a clear characterization of the dominant damage/failure mechanisms and their progressions can be formed.

MATERIAL AND TEST DETAILS

The TMC used in this study was SCS-6/Timetal[1] 21S $[0/90]_s$ with the fiber orientation designation indicating that the external most fibers were in the loading direction (i.e., the [0] orientation). SCS-6 is a SiC fiber with a nominal diameter of 140 μm. Timetal 21S is a metastable ß-titanium alloy with a nominal composition of Ti-15Mo-3Nb-3Al-0.2Si (wt. %). The TMC panel was fabricated by hot isostatic pressing alternate layers of Timetal 21S foil and SCS-6 fiber mat; TiNb ribbon was used as crossweave material in the fiber mats. The composite had a nominal fiber volume ratio of 39% and a nominal thickness of 0.85 mm. Coupon test specimens were cut from the panel using abrasive waterjet machining with no additional edge preparation. All specimens were subjected to a pre-test heat treatment, consisting of an 8 hour soak in vacuum at 621°C, to stabilize the ß+α microstructure of the Timetal 21S. The coupon specimen design [ref. 15] is a "dogbone" geometry featuring an overall length of 15.2 cm, a radius cut of 37 cm, and a central parallel-sided section of 2.6 cm. This design proved to be very successful at ensuring specimen failures within the controlled section. Tabs were attached to the specimen with adhesive for assembly purposes, and held in position by high clamping forces during the test.

All fatigue tests were conducted at 650°C in air on a closed-loop, computer-controlled, servo-hydraulic test system equipped with water-cooled grips. The load was controlled with a zero-tension (i.e., $R_\sigma = 0$) triangular command waveform cycled with a frequency of 1.0×10^{-2} Hz. Axial strain measurements were made over a centrally located 12.7 mm gage length with

[1]Timetal 21S is a registered trademark of TIMET, Titanium Metals Corporation.

a water-cooled extensometer mounted on the edge of the specimen. Radiant heating was provided to the specimen through the use of an inductively heated susceptor and intrinsic K-type thermocouples enabled temperature monitoring and closed-loop control. The thermocouple locations did not exhibit premature cracking and therefore were considered to have no influence on the specimen's fatigue life. Specimen failure is defined as complete fracture of the specimen into two pieces.

RESULTS AND DISCUSSION

Deformation

A representative tensile response of SCS-6/Timetal 21S $[0/90]_s$ at 650°C is shown in Fig. 1. In general, the stress-strain response exhibited an essentially linear portion up to approximately 125 MPa, at which point the response became non-linear with a gradually decreasing tangential stiffness with increasing load. The ultimate tensile strength and mechanical strain to failure were 690 MPa and 0.0095 m/m, respectively. With a thermal expansion strain from 25 to 650°C of 0.0044 m/m, the total composite strain at failure was 0.0139 m/m. Previous room temperature studies on similar TMCs have shown the tensile response to exhibit three distinct regions defined by two "knees" in the stress-strain behavior [refs. 16,17]. The first was an indication of F/M de-bonding in the [90] plies, and the second an indication of matrix plasticity in the [0] plies.

As-received thermal residual stresses have been estimated in a similar TMC through the use of a simple concentric cylinder model [ref. 18]. Results indicated that at relatively low temperatures, compressive radial and tensile hoop residual stresses in the titanium matrix provide a mechanical clamping force about the fiber. Thus, the position of the first knee in a room temperature test is a function of both the mechanical clamping force and the F/M bond strength. However, at temperatures above approximately 555°C (≈ ½ the matrix melting temperature), it is assumed that matrix stress relaxation essentially relieves the residual stresses, eliminating the mechanical clamping forces. Applying this interpretation to the 650°C tensile response shown in Fig. 1, the apparent proportional limit at approximately 125 MPa defines the point at which the physical bond fails at the [90] F/M interface. Beyond this composite stress, no distinct point in the curve suggests a specific event in one of the plies or constituents. However, it is noteworthy to cite that at this temperature the Timetal 21S matrix material will exhibit inelastic behavior at stresses as low as 20 MPa [ref. 19].

A representative fatigue deformation response at 650°C is shown in Fig. 2, where the maximum cyclic stress (S_{max}) was 450 MPa. Multiple cycles are shown to illustrate the progressive changes in deformation behavior up to two cycles before specimen failure. In comparison to subsequent cycles, initial cycles revealed the greatest degrees of inelastic behavior, with a "closed" hysteresis response not occurring until approximately cycle 10. Also, as revealed in the tensile response, the first cycle exhibited an initial linear portion to approximately 125 MPa. One measure of damage progression to note was the overall strain ratchetting which occurred prior to failure. This behavior was enabled due to the load-controlled conditions of the test. The representative test shown in Fig. 2 experienced an accumulated "permanent" strain (at zero load) of 0.0022 m/m prior to failure as indicated by cycle 2314. This strain ratchetting trend increased with increasing applied S_{max} as shown in Fig. 3 in terms of the maximum cyclic mechanical strain. These maximum strain increases, as well as the increases in cyclic strain range, are believed to be chiefly associated with matrix creep-relaxation behavior, additional F/M interface damage, and propagation of fatigue

cracks from the interfaces, but not a result of [0] fiber breakage (as the metallography will show). Note again the relatively low cyclic frequency of $1.0x10^{-2}$ Hz, as this test parameter is clearly relevant to the strain ratchetting behavior [ref. 6]. (This frequency was selected to enable subsequent comparisons to TMF deformation and damage [ref. 12]).

As a related issue concerning the deformation response, it is important to point out that in the presence of fatigue damage, the macroscopic coefficient of thermal expansion (CTE) of this material can change significantly [ref. 20]. Specifically, this cross-ply TMC will tend to exhibit a decreasing macroscopic CTE with fatigue damage accumulation [refs. 12,20]. A quantitative assessment of this effect under thermomechanical conditions revealed that this property changed by as much as 25%. Though the degradation of this property has not been quantified under 650°C isothermal conditions, it is reasonable to infer that the CTE has degraded, given that fatigue damage is clearly present (via many of the same damage mechanisms cited under TMF conditions). Further, numerical [ref. 21] and analytical [ref. 22] studies have conclusively shown that the macroscopic CTE of a composite laminate will degrade with damage (laminate cracking).

Consequently, it is erroneous to assume that the initial thermal strain component at 650°C (0.0044 m/m) remains constant throughout the isothermal test (as is commonly done), and thus, the reported mechanical strains, (calculated by subtracting the initial thermal strain from the total strain), will contain some degree of error. Note, however, that this will only affect the mechanical mean strain values and not the ranges. The only way to quantitatively correct the strain data for this effect is to periodically measure the thermal strain response during the test and account for it appropriately in the post-test data reduction. This measurement would have involved subjecting the specimen to periodic thermal cycling, and was therefore rejected, so as not to disturb the isothermal state of the specimen and introduce unwanted effects. The note is made here, however, for the sake of accuracy and data interpretation of Figs. 2 and 3.

Stiffness Degradation

In addition to the cyclic strain ratchetting behavior discussed above, stiffness degradation measurements also provide a quantitative means for tracking composite damage. Representative degradations of the composite stiffness (E_{650}) during cyclic fatigue at 650°C are shown in Fig. 4; four tests with different S_{max} values are presented. E_{650} values were calculated by taking the slope of a least-squared linear regression of the initial 25% of the cyclic unloads. As Fig. 4 indicates, the $[0/90]_s$ TMC system can experience significant stiffness reductions prior to failure. Composite stiffness degradation was found to increase with increasing S_{max}; this concurs with qualitative metallographic observations (discussed later) which revealed increased severity of matrix cracking with increased S_{max}. Note the extent of stiffness degradation incurred on the first cycle, where E_{650} of the specimen with S_{max} = 575 MPa exhibits an immediate 10% drop. First-cycle stiffness degradations such as these were not typically observed in comparable isothermal tests on unidirectional [0] TMCs [ref. 23], but rather, were distinctly observed in comparable tests on unidirectional [90] TMCs [refs. 8] where their drops were specifically associated with various states of F/M de-bonding. Further, metallographic evidence from specimens interrupted early in cyclic life reveal de-bonding of the [90] fibers, but a lack of [0] fiber cracking. Given this, and discounting matrix fatigue cracking at cycle 1, these varying degrees of first cycle stiffness loss are likely to be exclusively associated with de-bonding of the [90] ply.

Cyclic Life

Finally, in terms the macroscopic fatigue behavior, the resulting cyclic fatigue lives at 650°C are shown in Fig. 5. These and additional data are also given in Table 1. Also shown for comparison in Fig. 5 are the 650°C cyclic lives of the comparable [0] TMC (SCS-6/Timetal 21S $[0]_4$) generated by Russ and reported in ref. 24. As stated earlier, the [0/90] fatigue lives are significantly reduced from those exhibited by the [0] TMC; this to the extent that the [0/90] TMC lives are comparable to the [0] TMC lives at approximately ½ the level of S_{max}. The number of cycles to failure (N_f) decreases with increasing cyclic S_{max}, with the life trend at relatively high stresses exhibiting a very shallow slope. Here lives are essentially controlled by the excessive strain ratchetting rather than, for example, fatigue crack growth in the matrix. Note that a change of only 50 MPa, from a S_{max} of 625 to 575 MPa, causes N_f to change from 2 to 696 cycles, respectively. This type of high S_{max} strain ratchetting failure occurs in [0] unidirectional TMCs for many of the same matrix load shedding reasons, [refs. 23,25]; however, unlike the [0] TMC, it will be shown that [0] fiber cracks were not apparent in the [0/90] system. Below a S_{max} of approximately 550 MPa, mechanisms associated with fatigue crack growth in the matrix appear to dominate. The datum point with S_{max} = 350 MPa represents a specimen which did not fail after 29,000 cycles (33.5 days).

Fractography and Metallography

Fractography and metallography were conducted on several specimens taken from high, mid, and low cyclic S_{max} conditions investigated in this study. Fracture surfaces from all stress levels revealed environment assisted matrix cracking, with the exception of the S_{max} = 625 MPa test (N_f = 2 cycles) which revealed pure tensile overload. Oxidation patterns on the fracture surfaces such as the one shown in Fig. 6 suggested that the matrix cracks were internally initiated at the [90] F/M interfaces and propagated normal to the loading direction toward the [0] fibers. The severity of oxidation evident on the failure surface clearly increased with increased failure times (decreasing S_{max} levels). Based on the extent and location of internal oxidation, it was evident that the [90] fibers served as oxygen "conduits" enhancing internal environment assisted cracking. The fracture surfaces did not reveal any surface initiations. This observation was confirmed through SEM of the specimens' exterior surfaces and metallographic sectioning, as no surface cracking could be identified.

Metallographic sectioning clearly revealed a single dominant damage mode: environment assisted matrix cracking initiated at the [90] F/M interfaces, predominantly normal to the loading direction. This is illustrated in Figs. 7(a) and (b), where secondary cracks emanating from [90] fibers are viewed looking into the specimen's thickness. Sections taken from regions away from the fracture surfaces indicated that all [90] fibers exhibited some degree of F/M de-bonding. Qualitatively speaking, the severity of matrix cracking (with respect to size) visible on the various mounts increased with increasing S_{max}; however, the number of visible cracks did not significantly change with S_{max} level. As also shown in Fig. 7(a), several specimens exhibited [90] fiber damage; these cracks were most notable under mid to high S_{max} conditions. Control sections taken from untested specimens suggest that this fiber damage is not a result of the metallographic polishing. Note that these [90] fiber breaks appear as "splits" in this viewing plane; however, sections revealing the longitudinal axis of the [90] fibers also reveal breaks transverse to their longitudinal axis.

Longitudinal sections taken from the [0] plies revealed a consistent absence of [0] fiber cracking or de-bonding with one exception; [0] fiber interfaces in contact with the TiNb

crossweave ribbon exhibited localized de-bonding and oxidation. This pattern is illustrated in Fig. 8a with an un-etched mount, and also in Fig. 8b where the section has been etched with a lactic acid based etch to highlight the TiNb crossweave location. Note the correlation of the de-bonds with the crossweave ribbon which appears as white semi-circles in this plane. Although these localized de-bonds were present in all of the tests, they did not appear to promote preferential matrix cracking, except under relatively low stress (long life) conditions, where long term exposures enhanced the degree of localized oxidation, preferentially promoting matrix cracking at crossweave locations. This effect is best illustrated in Fig. 9 by the S_{max} = 350 MPa test which was interrupted after 33.5 days of testing (29000 cycles). Note the preferential damage associated with the highlighted TiNb crossweave locations, shown here associated with a [90] fiber ply.

SUMMARY/CONCLUSIONS

An experimental investigation was conducted to characterize the deformation, damage, and fatigue life of SCS-6/Timetal 21S $[0/90]_s$ under isothermal loadings at 650°C. The following summarizes the major findings:

- Initial failure of the [90] fiber/matrix (F/M) interface appeared to occur at approximately 125 MPa promoting measurable stiffness degradation.
- Fatigue degradations of the 650°C static moduli increased with increasing cyclic stress and provided a consistent measure of fatigue damage progression.
- The singular dominant damage was transverse matrix cracking initiated at [90] F/M interfaces; de-bonding of the [90] fibers was evident in all cases.
- Significant environment enhanced degradation was apparent and the exposed [90] fibers served to pipe oxygen along the internal F/M interfaces.
- De-bonding and environmental attack was enhanced at TiNb crossweave locations, but appeared to have a negative impact only under long term exposures.
- Neither surface initiated matrix cracking or [0] fiber cracking were apparent.

ACKNOWLEDGEMENTS

Thanks be to God. The author wishes to acknowledge Rod Ellis for his support and input to this research and Chris Burke, Ralph Corner, and Ron Shinn for their technical assistance in the Fatigue and Structures Laboratory and the Metallographic Laboratory at NASA Lewis Research Center.

REFERENCES

[1] Larsen, J.M., Russ, S.M. and Jones, J.W., "Possibilities and Pitfalls in Aerospace Applications of Titanium Matrix Composites," *NATO AGARD Conf. on Characterization of Fiber Reinforced Titanium Metal Matrix Composites*, Bordeaux, France, Sept. (1993).

[2] Lerch, B.A. and Saltsman, J.F., "Tensile Deformation of SiC/Ti-15-3 Laminates," *Composite Materials: Fatigue and Fracture Fourth Volume, ASTM STP 1156*, W.W. Stinchcomb & N.E. Ashbaugh, Philadelphia, (1993) pp. 161-175.

[3] Majumdar, B.S. and Newaz, G.M., "Inelastic Deformation of Metal Matrix Composites: Plasticity and Damage Mechanisms - Part II," NASA TM-189096, National Aeronautics and Space Administration, Washington, D.C., (1992).

[4] Pollock, W.D. and Johnson, W.S., "Characterization of Unnotched SCS-6/Ti-15-3 Metal Matrix Composites at 650°C," *Composite Materials: Testing and Design (Tenth Volume), ASTM STP 1120*, G.C. Grimes, Ed., Philadelphia (1992) pp. 175-191.

[5] Gayda, J. and Gabb, T.P., "Isothermal Fatigue Behavior of a $[90]_8$ SiC/Ti-15-3 Composite at 426°C," *International J. of Fatigue*, Jan. (1992) pp. 14-20.

[6] Mall, S. and Portner, B., "Characterization of Fatigue Behavior in Cross-Ply Laminate of SCS-6/Ti-15-3 Metal Matrix Composite at Elevated Temperature," *J. of Engineering Materials and Technology*, Vol. 114, Oct. (1992) pp. 409-415.

[7] Castelli, M.G. and Gayda, J., "An Overview of Elevated Temperature Damage Mechanisms and Fatigue Behavior of a Unidirectional SCS-6/Ti-15-3 Composite," *Reliability, Stress Analysis, and Failure Prevention*, DE-Vol. 55, ASME, Sept. (1993) pp. 213-221.

[8] Castelli, M.G., "Thermomechanical and Isothermal Fatigue Behavior of a $[90]_8$ Titanium Matrix Composite," In: *Proc. of The American Soc. for Composites 8th Tech. Conf. on Composite Material, Mechanics, and Processing*, Oct. (1993) pp. 884-892.

[9] Majumdar, B.S. and Newaz, G.M., "Thermomechanical Fatigue of a Quasi-Isotropic Metal Matrix Composite," *Composite Materials: Fatigue and Fracture (Third Volume), ASTM STP 1110*, T.K. O'Brien, Ed., Philadelphia, (1991) pp. 732-752.

[10] Mall, S. Hanson, D.G., Nicholas, T. and Russ, S.M., "Thermomechanical Fatigue Behavior of a Cross-Ply SCS-6/ß21-S Metal Matrix Composite," *Constitutive Behavior of High Temperature Composites*, MD-Vol. 40, B.S. Majumdar, G.M. Newaz and S. Mall, Eds. ASME, (1992) pp. 91-106.

[11] Russ, S.M. and Hanson, D.G., "Fatigue and Thermomechanical Fatigue of a SiC/Titanium $[0/90]_{2s}$ Composite," *Fatigue '93*, Vol. 2, J.P. Bailon and I.J. Dickson, Eds., Eng. Mat. Advisory Services, Ltd., U.K., (1993) pp. 1085-1090.

[12] Castelli, M.G., "Thermomechanical Fatigue Damage/Failure Mechanisms in SCS-6/Timetal 21S $[0/90]_s$ Composite," *Composites Engineering*, submitted for pub., (1994).

[13] Mirdamadi, M. and Johnson, W.S., "Stress-Strain Analysis of a $[0/90]_{2s}$ Titanium Matrix Laminate Subjected to a Generic Hypersonic Flight Profile," NASA TM 107584, National Aeronautics and Space Administration, Washington D.C., (1992).

[14] Neu, R.W. and Nicholas, T., " Effect of Laminate Orientation on the Thermomechanical Fatigue Behavior of Titanium Matrix Composites," *J. of Composites Technology and Research*, submitted for pub., (1993).

[15] Worthem, D.W., "Flat Tensile Specimen Design for Advanced Composites," NASA CR-185261, National Aeronautics and Space Administration, Washington D.C., (1990).

[16] Johnson, W.S., Lubowinski, S.J. and Highsmith, A. L., "Mechanical Characterization of SCS_6/Ti-15-3 Metal Matrix Composites at Room Temperature," *Thermal and Mechanical Behavior of Ceramic and Metal Matrix Composites, ASTM STP 1080*, J.M. Kennedy, H.H Moeller and W.S. Johnson, Eds., Philadelphia, (1990) pp. 451-489.

[17] Lerch, B.A., Melis, M.E. and Tong, M., "Experimental and Analytical Analysis of Stress-Strain Behavior in a $[0/90]_{2s}$ SiC/Ti-15-3 Laminate," NASA TM 104470, National Aeronautics and Space Administration, Washington D.C., (1991).

[18] Johnson, W.S., "Damage Development in Titanium Metal Matrix Composites Subjected to Cyclic Loading," *Composites*, Vol. 24, No. 3 (1993) pp. 187-196.

[19] Castelli, M.G., Arnold, S.M. and Saleeb, A.F., "Specialized Deformation Tests for the Characterization of a Viscoplastic Model: Application to a Titanium Alloy," NASA TM-106268, National Aeronautics and Space Administration, Washington, D.C., (1994).

[20] Castelli, M.G., "An Advanced Test Technique to Quantify Thermomechanical Fatigue Damage Accumulation in Composite Materials," *J. of Composites Technology and Research*, (in press, 1994).

[21] Herakovich, C.T. and Hyer, M.W., "Damage-Induced Property Changes in Composites Subjected to Cyclic Thermal Loading," *Engineering Fracture Mechanics*, Vol. 25 (1986), pp. 779-792.

[22] Hashin, Z. "Thermal Expansion Coefficients of Cracked Laminates," *Composites Science and Technology*, Vol 31 (1988), pp. 247-260.

[23] Castelli, M.G., Bartolotta, P.A. and Ellis, J.R., "Thermomechanical Testing of High-Temperature Composites: Thermomechanical Fatigue Behavior of SiC(SCS-6)/Ti-15-3," *Composite Materials: Testing and Design (Tenth Volume), ASTM STP 1120*, G.C. Grimes, Ed., Philadelphia, (1992) pp. 70-86.

[24] Neu, R.W. and Nicholas, T., "Life Prediction of SCS-6/Timetal 21S Under Thermomechanical Fatigue," *Thermomechanical Behavior of Advanced Structural Materials*, AD Vol. 34, W.F. Jones, Ed., ASME (1993), pp. 97-111.

[25] Gabb, T.P., Gayda, J., and MacKay, R.A., "Isothermal and Nonisothermal Fatigue Behavior of a Metal Matrix Composite," *J. of Composite Materials.*, Vol. 24 (1990) pp. 667–686.

S_{max} (MPa)	$\Delta\varepsilon$ at $\frac{1}{2}N_f$ (m/m)	Initial E_{650} (GPa)	N_f (cycles)
625	---	124	2
575	0.00616	129	696
550	0.00526	123	620
500	0.00484	121	1558
450	0.00429	128	2316
400	0.00384	127	6984
350	0.00329	123	29000^{+}

Table 1. Isothermal fatigue and material properties of SCS-6/Timetal 21S $[0/90]_s$ at 650°C.

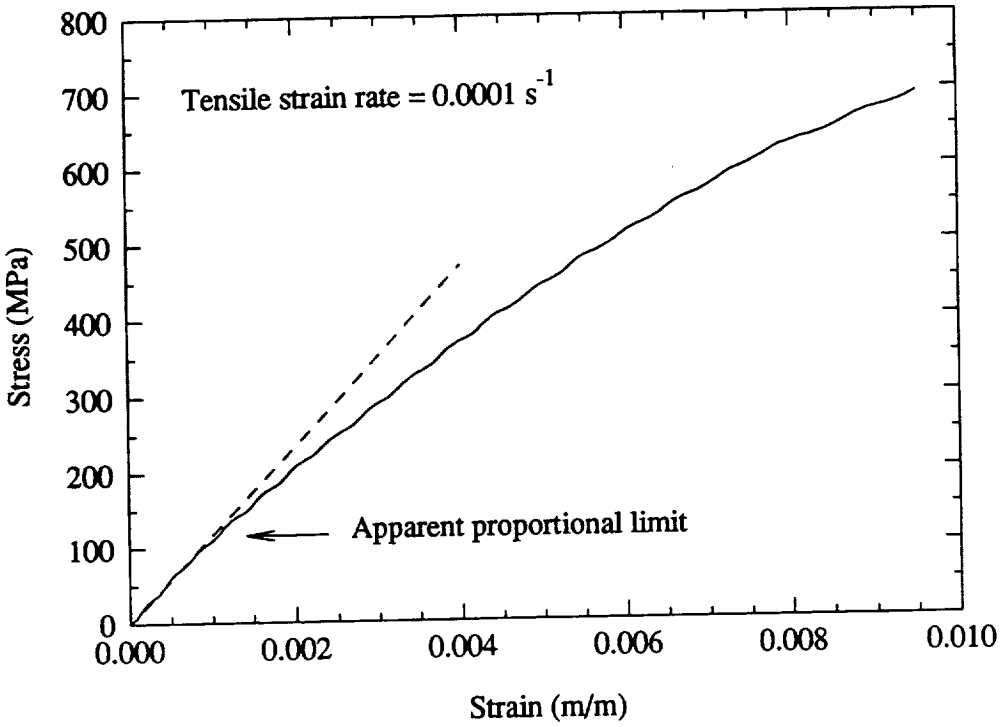

Figure 1. Representative tensile response of SCS-6/Timetal 21S $[0/90]_s$ at 650°C.

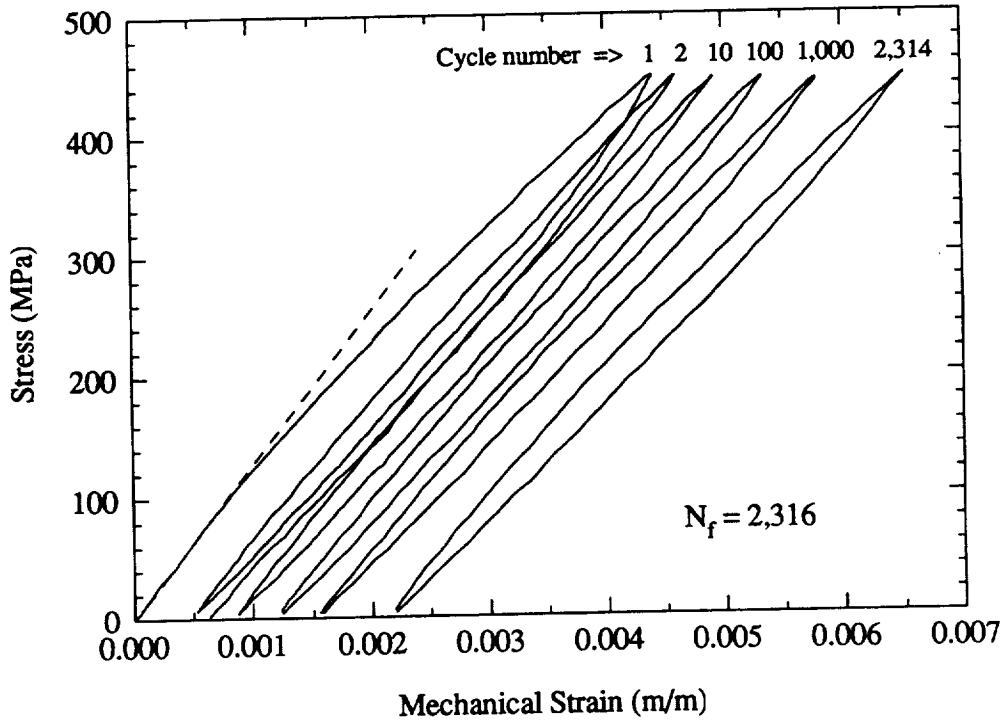

Figure 2. Deformation response of SCS-6/Timetal 21S $[0/90]_s$ at 650°C with S_{max} = 450 MPa.

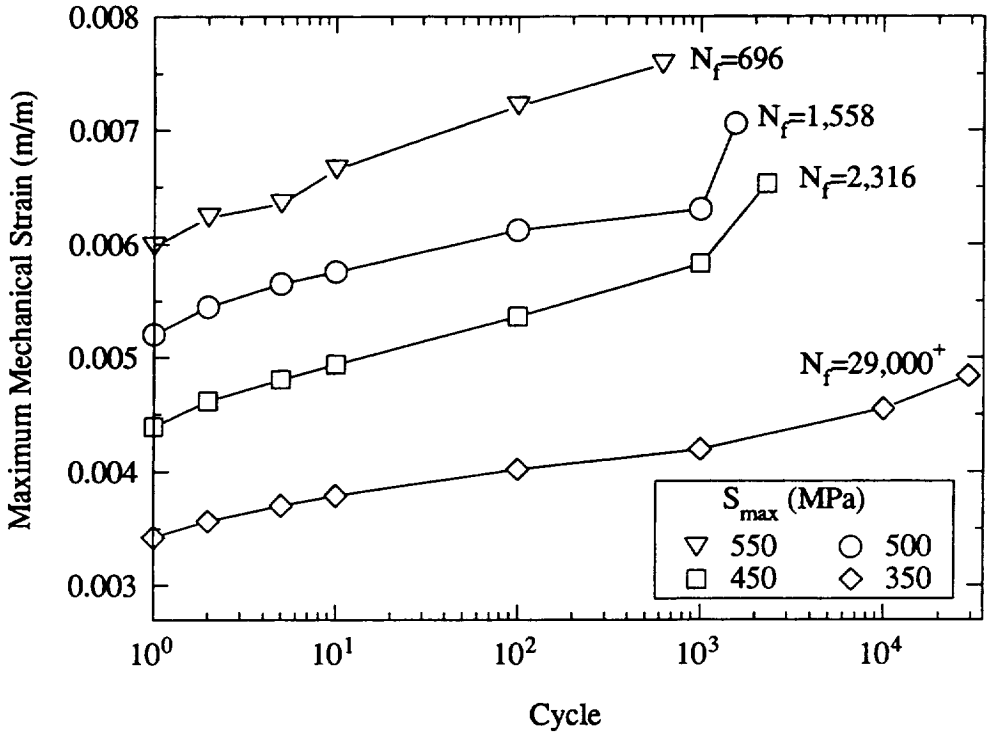

Figure 3. Maximum mechanical strain values illustrating the strain ratchetting behavior of SCS-6/Timetal 21S $[0/90]_s$ at 650°C.

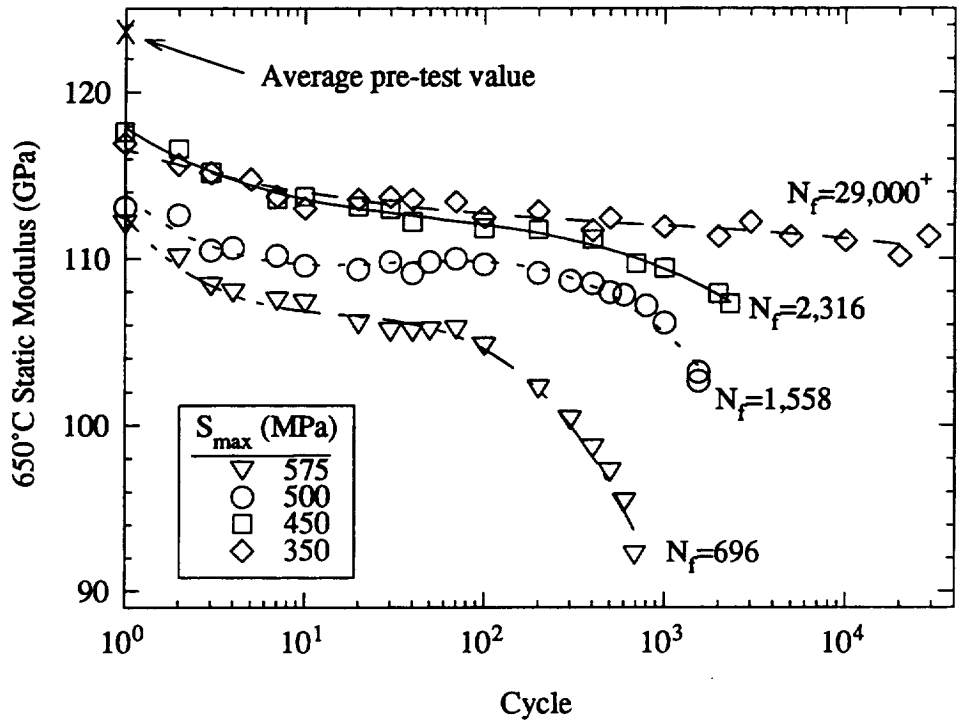

Figure 4. Degradation of the 650°C static modulus during 650°C isothermal fatigue of SCS-6/Timetal 21S $[0/90]_s$.

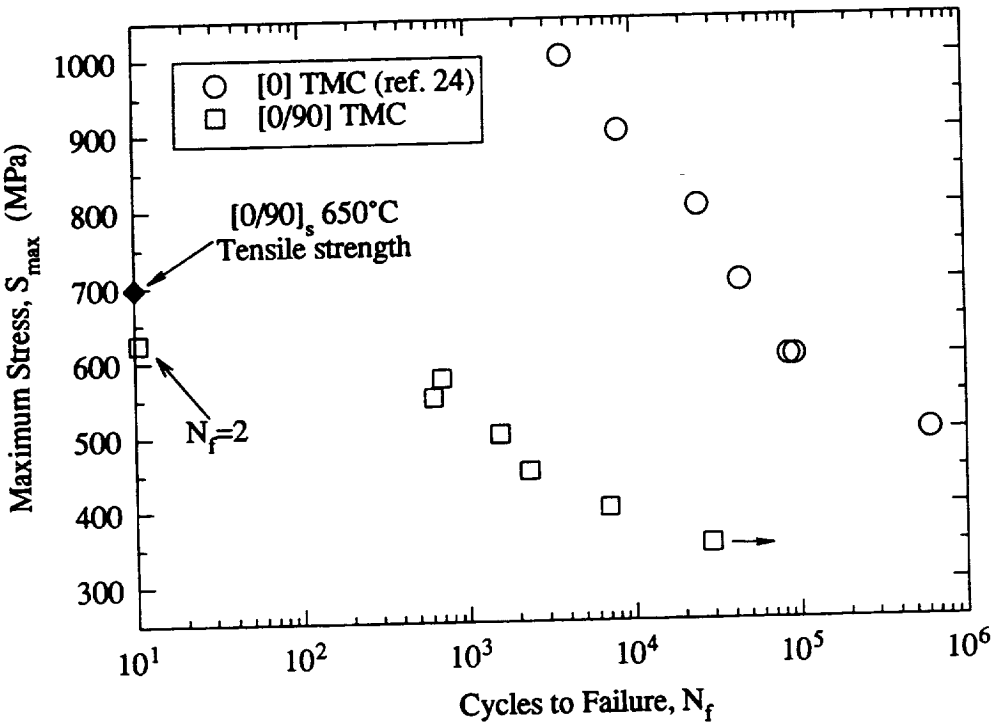

Figure 5. Isothermal fatigue life of SCS-6/Timetal 21S $[0]_4$ (ref. 24) and $[0/90]_s$ at 650°C.

S_{max} = 500 MPa, N_f = 1,558

200 μm

Figure 6. Fracture surface illustrating internal cracking with propagation toward external [0] fibers.

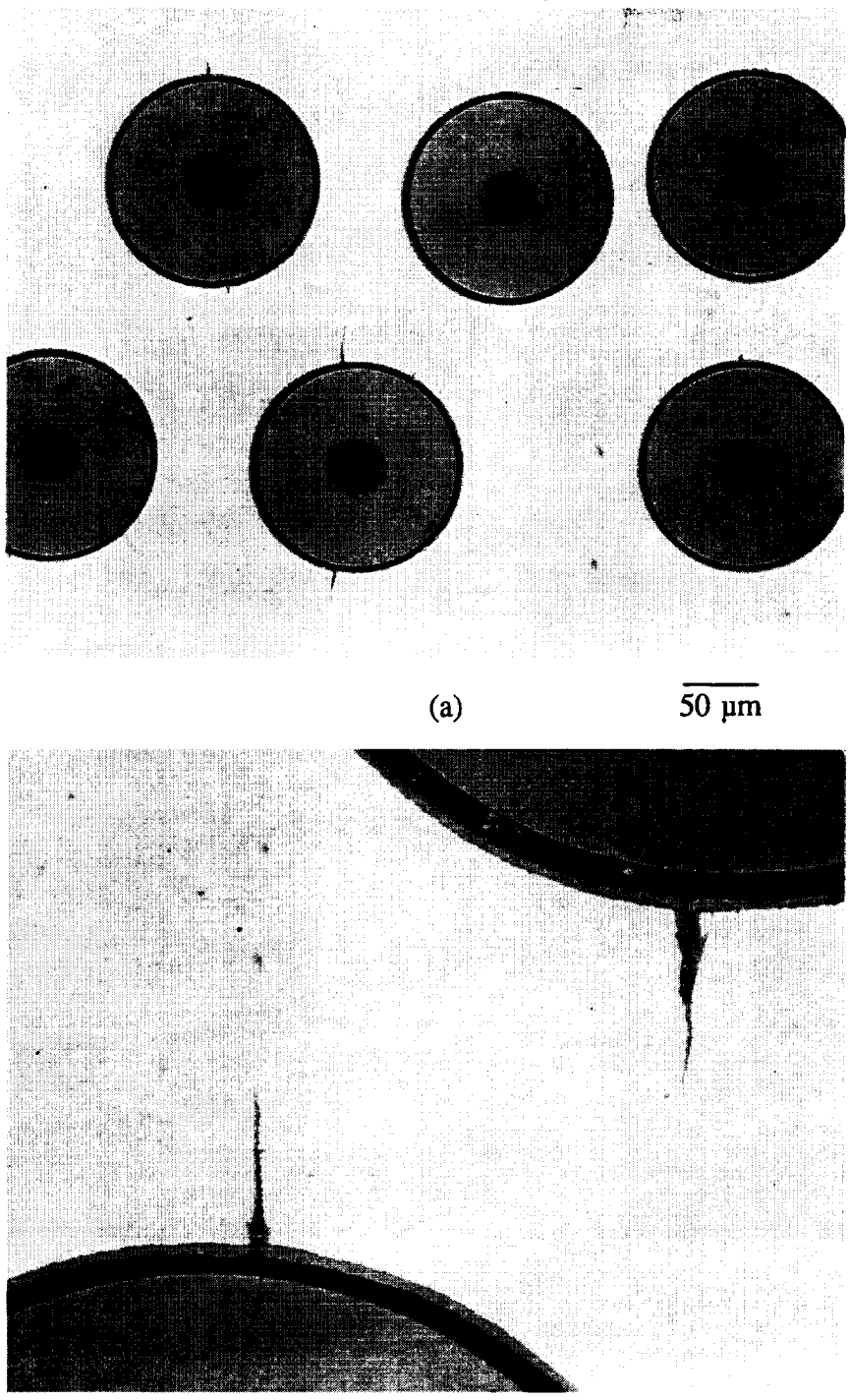

Figure 7. Metallographic sections showing secondary matrix cracks initiated at [90] F/M interface locations normal to the loading direction.

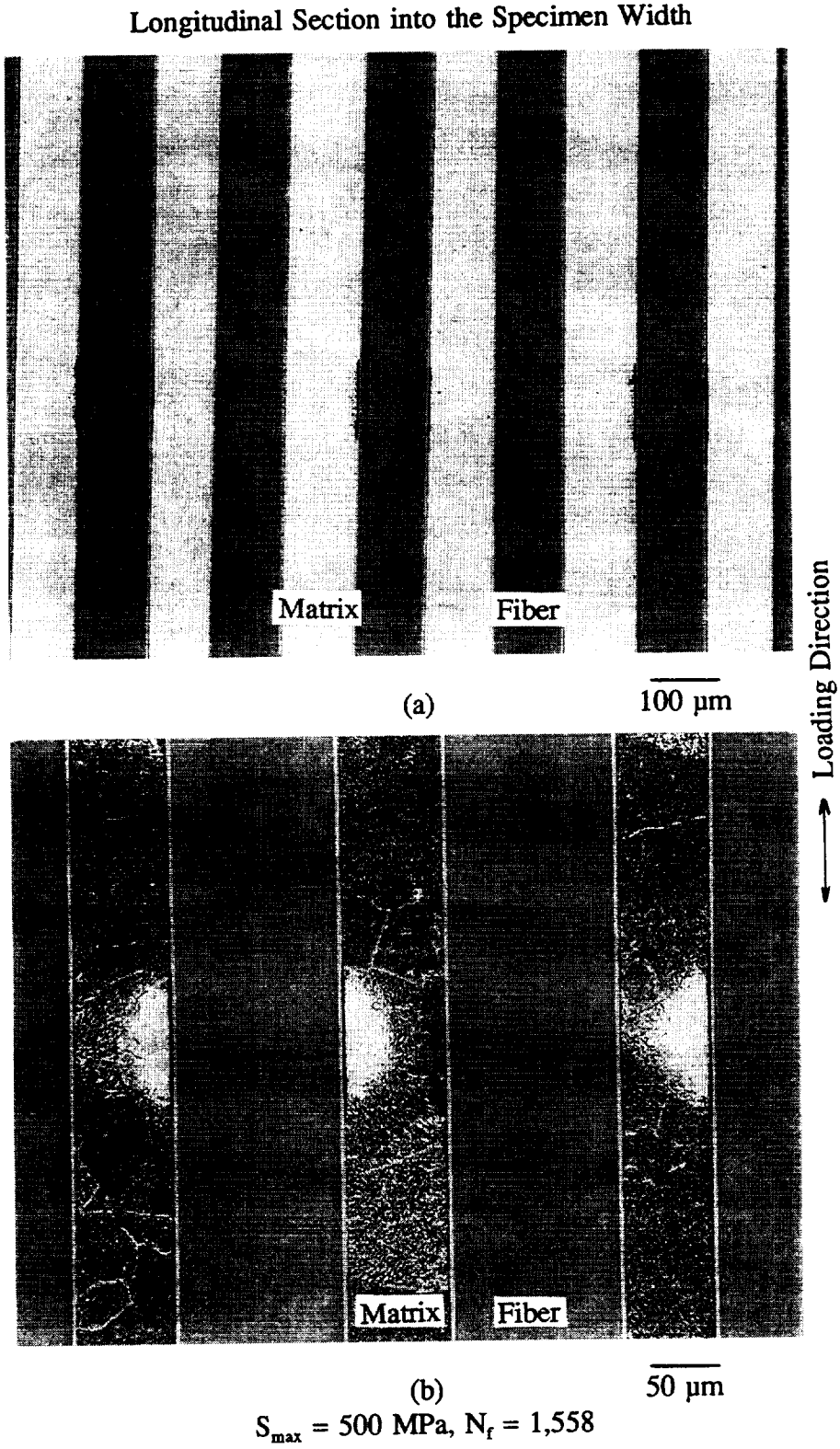

Figure 8. Metallographic sections, (a) un-etched, and (b) etched, of [0] fibers illustrating de-bonds and enhanced oxidation at TiNb crossweave locations.

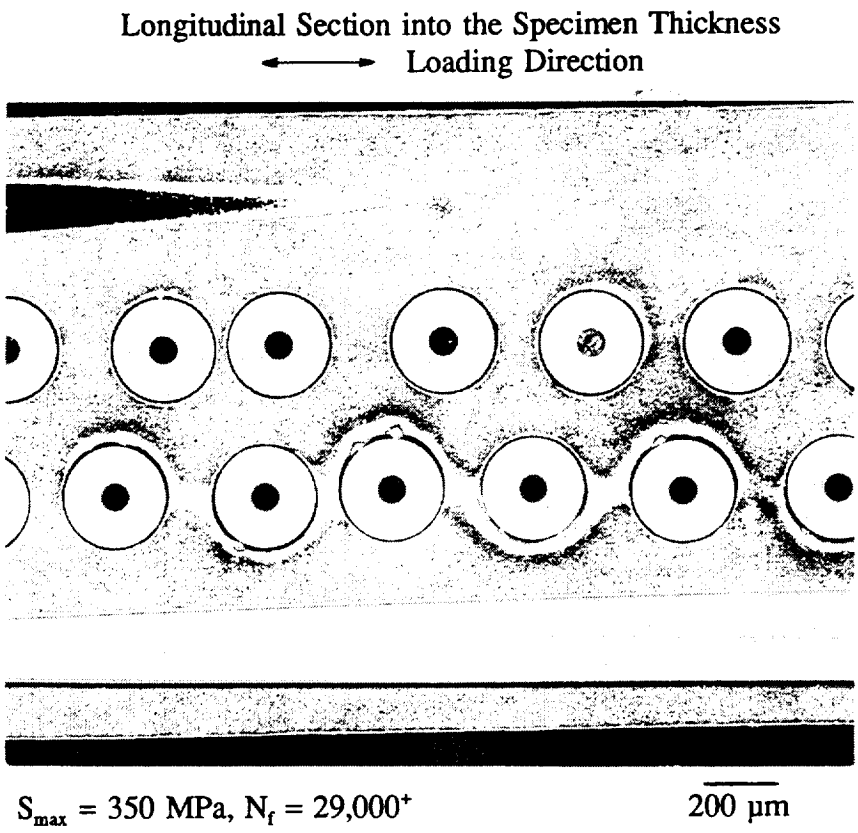

Figure 9. Etched metallographic section illustrating enhanced oxidation and matrix cracking at [90] fiber and TiNb crossweave locations.

REPORT DOCUMENTATION PAGE

Form Approved
OMB No. 0704-0188

1. AGENCY USE ONLY (*Leave blank*)	2. REPORT DATE	3. REPORT TYPE AND DATES COVERED
	June 1994	Final Contractor Report

4. TITLE AND SUBTITLE

Isothermal Damage and Fatigue Behavior of SCS-6/Timetal 21S [0/90]s Composite at 650°C

5. FUNDING NUMBERS

WU-763-22-41
C-NAS3-27186

6. AUTHOR(S)

Michael G. Castelli

7. PERFORMING ORGANIZATION NAME(S) AND ADDRESS(ES)

NYMA, Inc.
Engineering Services Division
2001 Aerospace Parkway
Brook Park, Ohio 44142

8. PERFORMING ORGANIZATION REPORT NUMBER

E-8927

9. SPONSORING/MONITORING AGENCY NAME(S) AND ADDRESS(ES)

National Aeronautics and Space Administration
Lewis Research Center
Cleveland, Ohio 44135-3191

10. SPONSORING/MONITORING AGENCY REPORT NUMBER

NASA CR-195345

11. SUPPLEMENTARY NOTES

Project Manager, Rod Ellis, Structures Division, NASA Lewis Research Center, organization code 5220, (216) 433-3340.

12a. DISTRIBUTION/AVAILABILITY STATEMENT

Unclassified - Unlimited
Subject Category 24

12b. DISTRIBUTION CODE

13. ABSTRACT (***Maximum 200 words***)

The isothermal fatigue damage and life behaviors of SCS-6/Timetal 21S [0/90]s were investigated at 650°C. Strain ratchetting and degradation of the composite's static elastic modulus were carefully monitored as functions of cycles to indicate damage progression. Extensive fractographic and metallographic analyses were conducted to determine damage/failure mechanisms. Resulting fatigue lives show considerable reductions in comparison to [0] reinforced titanium matrix composites subjected to comparable conditions. Notable stiffness degradations were found to occur after the first cycle of loading, even at relatively low maximum stress levels, where cyclic lives are greater than 25,000 cycles. This was attributed to the extremely weak fiber/matrix bond which fails under relatively low transverse loads. Stiffness degradations incurred on first cycle loadings and degradations thereafter were found to increase with increasing maximum stress. Environmental effects associated with oxidation of the [90] fiber interfaces clearly played a role in the damage mechanisms as fracture surfaces revealed environment assisted matrix cracking along the [90] fibers. Metallographic analysis indicated that all observable matrix fatigue cracks initiated at the [90] fiber/matrix interfaces. Global de-bonding in the loading direction was found along the [90] fibers. No surface initiated cracks were evident and minimal if any [0] fiber cracking was visible.

14. SUBJECT TERMS

Titanium matrix composites; Fatigue behavior; Damage mechanisms; Metallographic analysis; Stiffness loss

15. NUMBER OF PAGES

17

16. PRICE CODE

A03

17. SECURITY CLASSIFICATION OF REPORT	18. SECURITY CLASSIFICATION OF THIS PAGE	19. SECURITY CLASSIFICATION OF ABSTRACT	20. LIMITATION OF ABSTRACT
Unclassified	Unclassified	Unclassified	

National Aeronautics and
Space Administration
Lewis Research Center
21000 Brookpark Rd.
Cleveland, OH 44135-3191